THE JOURNAL OF BIOLOGICAL CHEMISTRY VOL. 286, NO. 23, pp. 20615–20624, June 10, 2011

Thymidine Analogue Excision and Discrimination Modulated by Mutational Complexes Including Single Amino Acid Deletions of Asp-67 or Thr-69 in HIV-1 Reverse Transcriptase*[S]

Received for publication, January 28, 2011, and in revised form, April 16, 2011 Published, JBC Papers in Press, April 19, 2011, DOI 10.1074/jbc.M111.226100

Mónica Kisic[‡1], Tania Matamoros[‡1], María Nevot[§], Jesús Mendieta[‡], Javier Martinez-Picado[§¶], Miguel A. Martínez[§], and Luis Menéndez-Arias[‡2]

From the [‡]Centro de Biología Molecular "Severo Ochoa", Consejo Superior de Investigaciones Científicas and Universidad Autónoma de Madrid, 28049 Madrid, Spain and the [§]Laboratori de Retrovirologia, Fundació irsiCaixa, Hospital Universitari Germans Trias i Pujol, Badalona, 08916 Barcelona, Spain, and the [¶]Institució Catalana de Recerca i Estudis Avançats, 08010 Barcelona, Spain

Single amino acid deletions in the β3-β4 hairpin loop of human immunodeficiency virus type 1 (HIV-1) reverse transcriptase (RT) have been identified in heavily treated patients. The deletion of Asp-67 together with mutations T69G and K70R (Δ67 complex) are usually associated with thymidine analog resistance mutations (TAMs) (*e.g.* M41L, T215Y, etc.) while the deletion of Thr-69 (Δ69) is rarely found in isolates containing TAMs. Here, we show that the complex Δ67/T69G/K70R enhances ATP-dependent phosphorolytic activity on primers terminated with 3′-azido-3′-deoxythymidine (AZT) or 2′,3′-didehydro-2′,3′-dideoxythymidine (d4T) both in the presence or absence of TAMs (*i.e.* M41L/T215Y), while Δ69 (or the complex S68G/Δ69/K70G) antagonize the effects of TAMs in ATP-mediated excision. These effects are consistent with AZT susceptibility data obtained with recombinant HIV-1 bearing the relevant RTs. Molecular dynamics studies based on models of wild-type HIV-1 RT and mutant Δ69, Δ67/T69G/K70R, and D67N/K70R RTs support a relevant role for Lys/Arg-70 in the excision reaction. In Δ69 RT, the side chain of Lys-70 locates away from the putative pyrophosphate binding site. Therefore, its participation in interactions required for the excision reaction is unlikely. Our theoretical studies also suggest a role for Lys-219 in thymidine analog excision/discrimination. However, pre-steady-state kinetics revealed only minor differences in selectivity of AZT-triphosphate *versus* dTTP between deletion-containing RTs and their homologous enzymes having the K219E mutation. K219E reduced both ATP- and pyrophosphate-mediated excision of primers terminated with thymidine analogues, only when introduced in RTs bearing Δ69 or S68G/Δ69/K70G, providing further biochemical evidence that explains the lack of association of Δ69 and TAMs in HIV-1 isolates.

The human immunodeficiency virus type 1 (HIV-1) reverse transcriptase (RT) is a heterodimeric enzyme that converts the single-stranded viral genomic RNA into double-stranded DNA, which is integrated into the host genome (1, 2). HIV-1 RT is composed of subunits of 560 and 440 residues, designated as p66 and p51, respectively. Both subunits have identical amino acid sequence, but p51 lacks residues 441–560 of p66, because they are removed by the HIV-1 protease during virus maturation. The DNA polymerase active site resides within the palm subdomain of p66, which contains the essential catalytic aspartic acid residues 110, 185, and 186. HIV-1 RT is a major target for chemotherapeutic intervention in the control of AIDS. Drugs targeting this viral enzyme include nucleoside/nucleotide RT inhibitors (NRTIs)[3] and nonnucleoside RT inhibitors (NNRTIs) (3, 4). NRTIs (*e.g.* zidovudine, lamivudine, stavudine, etc.) have to be converted to their triphosphate derivatives to be incorporated into the nascent DNA by the viral RT. Because NRTIs lack a 3′-OH group their incorporation results in chain termination.

There are two major mechanisms of HIV resistance to NRTIs (reviewed in Refs. 1, 5). One of them is based on nucleotide selectivity, and is exemplified by lamivudine-resistance mutations M184V and M184I, and by the Q151M complex (A62V/V75I/F77L/F116Y/Q151M) that confers resistance to multiple NRTIs (6, 7). These amino acid substitutions affect residues of the dNTP binding site of the RT (8), while reducing the enzyme's ability to incorporate the triphosphorylated NRTIs. The second mechanism involves enhanced excision of the

* This work was supported by grants of the Ministry of Science and Innovation of Spain (BIO2010/15542), Fundación para la Investigación y Prevención del SIDA en España (FIPSE) (Grant 36771/08), Fondo de Investigación Sanitaria (through the "Red Temática de Investigación Cooperativa en SIDA" RD06/006), and an institutional grant from the Fundación Ramón Areces. Work at Fundació irsiCaixa was supported by Spanish Ministry of Science and Innovation Grant BFU2010-15194 (to M. A. M.), and by the European Community's Seventh Framework Program (FP7/2007-2013) under the project "Collaborative HIV and Anti-HIV Drug Resistance Network (CHAIN)."

[S] The on-line version of this article (available at http://www.jbc.org) contains supplemental Figs. S1–S4 and Tables S1 and S2.

[1] Both authors contributed equally to this work.

[2] To whom correspondence should be addressed: Centro de Biología Molecular "Severo Ochoa" (CSIC-UAM), c/Nicolás Cabrera, 1, Campus de Cantoblanco, 28049, Madrid, Spain. Tel.: 34-911964494; Fax: 34-911964420; E-mail: lmenendez@cbm.uam.es.

[3] The abbreviations used are: NRTIs, nucleoside RT inhibitors; PP_i, pyrophosphate; TAM, thymidine analogue resistance mutation; AZT, 3′-azido-3′-deoxythymidine; d4T, 2′,3′-didehydro-2′,3′-dideoxythymidine; 3TC, β-L-(−)-2′,3′-dideoxy-3′-thiacytidine; TP, triphosphate; dsDNA, double-stranded DNA; MP, monophosphate.

chain-terminating NRTI from the 3′-end of the blocked primer, using ATP as pyrophosphate (PP_i) donor (9). Unblocking the primer allows RT to continue DNA synthesis. Available data indicate that thymidine analogues (*i.e.* zidovudine or stavudine) and tenofovir are the best substrates of the reaction (9–13). Mutations commonly associated with excision-mediated resistance are M41L, D67N, K70R, L210W, T215F/Y, and K219E/Q (14–18). These mutations are usually known as thymidine analog resistance mutations (TAMs) and emerge after long-term therapy with β-D-(+)-3′-azido-3′-deoxythymidine (AZT, zidovudine) and/or β-D-(+)-2′,3′-didehydro-2′,3′-dideoxythymidine (d4T, stavudine). The accumulation of three or more TAMs confers resistance to all clinically approved RT inhibitors.

Insertions of one or two amino acids, as well as single amino acid deletions in the β3-β4 hairpin loop (residues 64–72), are frequently found in heavily mutated multidrug-resistant HIV-1 isolates from patients that do not respond to the available therapies (19, 20). The prevalence of β3-β4 hairpin loop deletions has been estimated to be less than 0.2% among patients failing antiretroviral treatment including NRTIs (21, 22). These deletions may appear together with mutations of the Q151M complex or with TAMs. The deletion of RT codon 69 (encoding for Thr-69) has been observed in combination with one or more mutations of the Q151M complex in viral isolates resistant to multiple NRTIs (21, 23). The 69 deletion (Δ69) alone confers AZT hypersusceptibility and resistance to β-L-(−)-2′,3′-dideoxy-3′-thiacytidine (3TC, lamivudine) in phenotypic assays (23). Biochemical studies have shown that in the absence of TAMs, Δ69 decreases ATP-mediated excision of primers terminated with AZT as well as the catalytic efficiency of incorporation of 3TC triphosphate (3TCTP) relative to dCTP by the HIV-1 RT (24).

Viral isolates lacking the RT codon 67 (Asp-67) showed high level resistance to AZT in phenotypic assays, although their decreased susceptibility could be attributed to the simultaneous presence of TAMs (25). In the absence of TAMs, the combination of the 67 deletion (Δ67) and T69G confers low-level resistance to d4T, 3TC and abacavir but retains susceptibility to AZT and didanosine (21, 25, 26). Recombinant HIV-1 RTs with complex mutational patterns including Δ67 (*e.g.* M41L/Δ67/T69G/K70R/L74I/K103N/T215Y/K219Q) showed high-level excision activity on primers terminated with AZT, d4T or tenofovir, particularly in the presence of PP_i (27). However, the contribution of excision and nucleotide discrimination mechanisms to resistance mediated by Δ67 has not been studied in detail.

In this work, a genotypic analysis of HIV-1 *pol* sequences of isolates from treated patients shows that there are two major mutational complexes associated with single amino acid deletions at codons 67 or 69 in the β3-β4 hairpin loop of the RT. The Δ67 complex (*i.e.* Δ67/T69G/K70R) is usually found together with TAMs, while these mutations are rare when Δ69 is present, as for example, in the case of the S68G/Δ69/K70G complex. In previous studies we showed the selection of this mutational complex in a heavily treated patient, infected with drug-resistant HIV-1 bearing mutations A62V, V75I, F77L, F116Y, and Q151M in the RT (23).

Now, we have analyzed the contribution to NRTI excision of such mutational complexes in the presence or absence of TAMs, as well as their role in discriminating against AZT triphosphate (AZTTP). Crystallographic data (8, 28) and molecular dynamics studies (24) suggested an interaction between loops β3-β4 and β11a-β12, including Lys-219. In the crystal structure of HIV-1 RT complexed with dsDNA and dNTP (8), the side chain of Lys-219 interacts with the side chain of Asp-67, but this interaction is predicted to be lost in the presence of Δ69 (24), suggesting a role for this residue in NRTI excision/incorporation. Recombinant RTs bearing K219E showed altered nucleotide selectivity in the presence of any of both deletion complexes, but decreased ATP-mediated excision only when Δ69 was present.

MATERIALS AND METHODS

Reverse Transcriptases—Wild-type (WT) HIV-1_{NL4-3} and HIV-1_{BH10} RTs, and mutant derivatives Δ69 (HIV-1_{NL4-3} RT lacking Thr-69) and M41L/T215Y (in an HIV-1_{BH10} RT background) were obtained as previously described, using modified versions of plasmid p66RTB (24, 29). Other mutants were obtained by using the QuikChange site-directed mutagenesis kit (Stratagene), following the manufacturer's instructions. Template and primers used in the mutagenesis reaction are given in the supplemental Table S1. Mutant RTs Δ67/T69G/K70R/K219E and S68G/Δ69/K70G/K219E were obtained by introducing the substitution K219E, in previously generated plasmids containing Δ67/T69G/K70R and S68G/Δ69/K70G, respectively. The Δ67 mutant was obtained by reverting to WT sequence the mutations found at positions 69 and 70 in Δ67/T69G/K70R. All constructs were verified by restriction enzyme analysis and nucleotide sequencing (Macrogen Inc., Seoul, South Korea).

Recombinant heterodimeric RTs were expressed and purified as previously described (30, 31). RT p66 subunits carrying a His_6 tag at their C terminus were co-expressed with HIV-1 protease in *Escherichia coli* XL1 Blue to obtain p66/p51 heterodimers, which were later purified by ionic exchange followed by affinity chromatography. Enzymes were quantified by active site titration (31, 32), before biochemical studies.

Nucleotides and Template/Primers—Stock solutions (100 mM) of dNTPs and rNTPs were obtained from GE Healthcare. AZTTP and d4T triphosphate (d4TTP) were obtained from Trilink BioTechnologies (San Diego, CA) and Sierra Bioresearch (Tucson, AZ), respectively. Before use, nucleoside-TPs were treated with inorganic pyrophosphatase to remove traces of PP_i (13). DNA oligonucleotides 21P (3′-CCTATGTATACCAATTTCATA-5′), 31T (3′-TATGAAATTGGTATACATAGGATTTTTTTTT-5′), 25PGA (3′-GGACGTTCTTACATATCGGGATGGT-5′), and D38 (3′-ACCATCCCGATATGTAAGAACGTCCATTCTTTCCTGGG-5′) were obtained from Invitrogen. Oligonucleotides 21P and 25PGA were labeled at their 5′ termini with [γ-^{32}P]ATP (Perkin Elmer) and T4 polynucleotide kinase (New England Biolabs) in 70 mM Tris-HCl (pH 7.5) buffer, containing 10 mM $MgCl_2$ and 5 mM dithiothreitol. Annealing of template/primers 31T/21P and D38/25PGA was carried out as described (33, 34).

Pre-steady-state Kinetic Assays—Transient kinetic parameters for nucleotide incorporation were determined with a rapid quench instrument (model QFM-400, Bio-Logic Science Instruments, Claix, France) with reaction times ranging from 10 ms to 6 s (35). For the incorporation of dTTP, reactions were performed at 37 °C by mixing 16 μl of a solution containing 100 nM (active sites) of the corresponding RT and 200 nM of the template/primer 31T/21P in RT buffer (50 mM Tris-HCl, pH 8.0; 50 mM KCl) with 16 μl of RT buffer containing variable amounts of dNTP in 25 mM $MgCl_2$. Reactions involving AZTTP were conducted under the same conditions with excess concentrations of enzyme (200 nM) over the template/primer duplex (100 nM). All reactions were stopped with 0.3 M EDTA (final concentration). Aliquots of the reaction products were mixed with equal amounts of a solution containing 10 mM EDTA in 90% (v/v) formamide containing 3 mg/ml of xylene cyanol FF and 3 mg/ml of bromophenol blue. Products were analyzed by sequencing gel electrophoresis (20% (w/v) polyacrylamide/8 M urea in Tris borate-EDTA buffer) and quantified by phosphorimaging with a BAS 1500 scanner (Fuji), using the program Tina version 2.09 (Raytest Isotopenmessgerate Gmbh, Staubenhardt, Germany). The formation of product [*P*] over time was fitted with burst Equation 1,

$$[P] = A \times [1 - \exp(-k_{obs} \times t)] + k_{ss} \times t \qquad \text{(Eq. 1)}$$

where A is the amplitude of the burst, k_{obs} is the apparent kinetic constant of formation of the phosphodiester bond, and k_{ss} is the enzyme turnover rate (*i.e.* the kinetic constant of the steady-state linear phase). The dependence of k_{obs} on dNTP concentration is described by the hyperbolic Equation 2,

$$k_{obs} = k_{pol} \times [\text{dNTP}]/(K_d + [\text{dNTP}]) \qquad \text{(Eq. 2)}$$

where K_d and k_{pol} are the equilibrium and the catalytic rate constants of the dNTP for RT, respectively. K_d and k_{pol} were determined from curve fitting using Sigma Plot.

Chain Terminator Excision Assays—RT-catalyzed DNA rescue reactions were performed with template/primer D38/25PGA as described (24, 36). Briefly, the DNA duplex containing the phosphorylated primer (30 nM) and the corresponding RT were preincubated at 37 °C for 10 min in 20 μl of 50 mM Hepes buffer (pH 7.0) containing 15 mM NaCl, 15 mM magnesium acetate, 130 mM potassium acetate, 1 mM dithiothreitol, and 5% (w/v) polyethylene glycol 6000. Reactions were initiated by adding 20 μl of preincubation buffer containing 50 μM AZTTP or d4TTP, depending on the assay. After incubating the samples at 37 °C for 30 min, the rescue reactions were carried out by adding 40 μl to a mixture of all dNTPs, and the corresponding PP_i donor, in the buffer indicated above. PP_i donors used were sodium PP_i (at 200 μM), ATP (at 3.2 mM) or GTP (at 9.6 mM). In these assays, all dNTPs except dATP were supplied at a final concentration of 100 μM. Because the next complementary dNTP (dATP in our assay conditions) has an inhibitory effect on the reaction, time course experiments of the unblocking and extension reactions were carried out with 1 μM dATP. Active RT concentrations in these assays were in the range of 24 to 72 nM. Rescue reactions were incubated for up to 150 min, and aliquots of 4 μl were removed at appropriate times and added to 12 μl of EDTA/formamide stop solution. Products were then resolved on denaturing polyacrylamide-urea gels and primer rescue was quantified by phosphorimaging.

Homology Modeling and Molecular Dynamics—Structural models of mutant RTs Δ67/T69G/K70R and D67N/K70R were constructed by standard homology modeling techniques (24). Molecular dynamics simulations, based on the model, were performed as previously described for the WT HIV-1 RT (34). The system included the DNA polymerase domain (residues 1–389) of the 66 kDa subunit of the RT, a 15/12-mer DNA/DNA template/primer and residues 3–82 of the 51-kDa subunit of the RT. Two Mg^{2+} ions and the incoming dNTP were also included in the system. The total simulation length was around 10 ns, and the analysis of trajectories was performed as described (34).

HIV Drug Susceptibility Tests—Resistance to RT inhibitors was determined with a drug susceptibility assay involving the generation of recombinant HIV-1 variants after co-transfecting MT-4 cells with a PCR product containing the RT coding sequence DNA and an RT-deleted HXB2-D clone previously linearized with BstEII (37). The MT-4 cells and the deleted HXB2-D clone were obtained from the AIDS Reagent Program (Medical Research Council). RT inhibitors and ritonavir were obtained from the NIH AIDS Research and Reference Reagent Program. After virus propagation and titration, HIV-1 drug susceptibility data were obtained in MT-4 cells as previously described (29).

RESULTS

Mutations Associated with Deletions in the β3-β4 Hairpin Loop of the RT—The prevalence of deletions in the RT fingers subdomain has been estimated to be less than 0.2% in HIV-infected patients, treated with nucleoside inhibitors (21, 22). After searching the Stanford HIV Drug Resistance database, we identified 68 RT sequences containing three-nucleotide deletions in the β3-β4 hairpin loop. Amino acid sequence alignments of the region comprising RT residues 41–220 showed that about one-third of the sequences lacked Asp-67 (or any other acidic residue at positions 64–72) (supplemental Fig. S1). Most of them shared a consensus sequence KKKSGRWR (Δ67/T69G/K70R) for positions 64–72 at the tip of the β3-β4 hairpin loop. On the other hand, sixty percent of the deletion-containing RTs contained Asp-67, and had a consensus sequence KKKDGKWR (S68G/Δ69) at positions 64–72. TAMs were commonly found in the sequences lacking Asp-67. Thus, 69.6% of these sequences contained M41L and 87% contained T215Y. Mutations of the Q151M complex were rarely identified in RTs lacking Asp-67, but K219E or K219Q were found in 22 out of the 23 sequences analyzed. In contrast, 40% of the RTs with the consensus sequence KKKDGKWR (S68G/Δ69) contained Q151M, while TAMs were rarely observed in this group of sequences.

Effects of Δ67 and Δ69 on the Excision Activity of WT and Mutant RTs—The ability of RTs to rescue AZT monophosphate (AZTMP)- and d4T monophosphate (d4TMP)-terminated primers was assessed by using the template/primer shown in Fig. 1*A*. These experiments were carried out in two steps. First, the enzyme and the template/primer were incu-

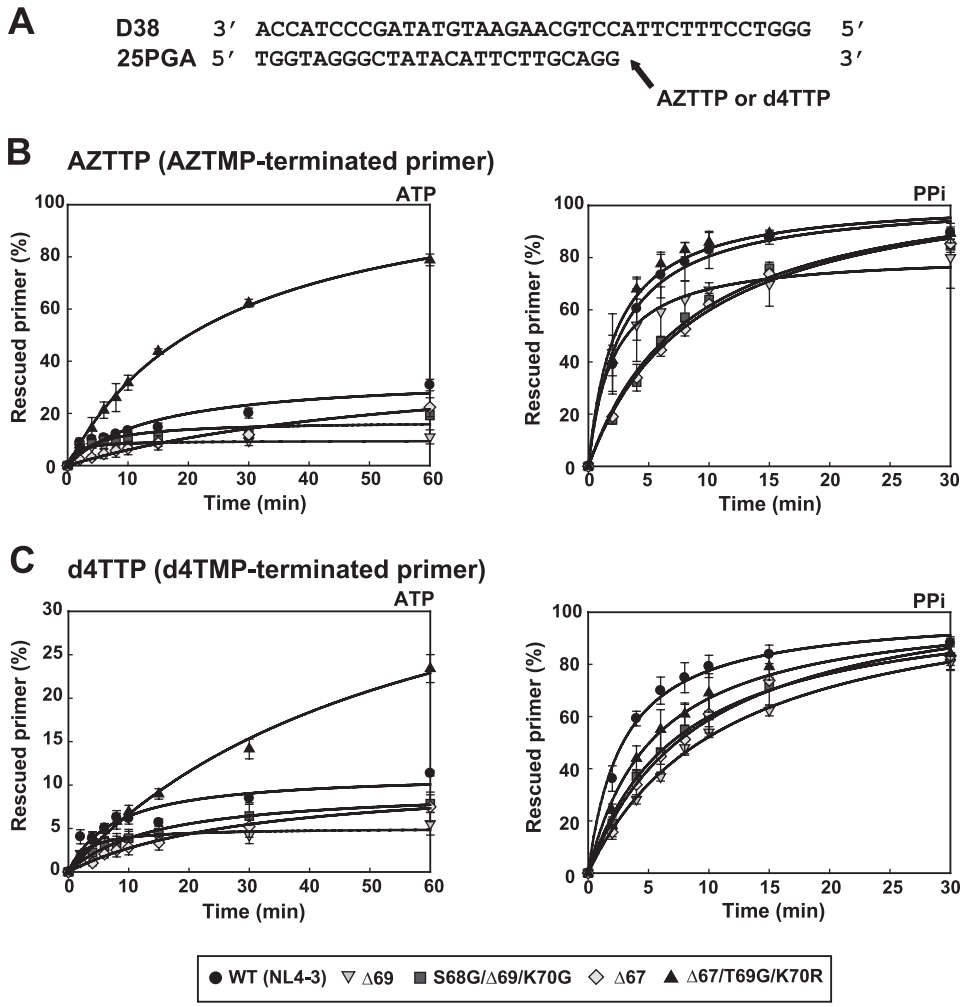

FIGURE 1. **Rescue DNA polymerization reactions catalyzed by WT and mutant RTs and initiated from primers terminated with AZTMP or d4TMP.** Assays were carried out with the heteropolymeric template/primer D38/25PGA whose sequence is given in *panel A*. Time courses of AZTMP (*B*) and d4TMP (*C*) excision reactions carried out in the presence of 3.2 mM ATP (*left*) or 200 μM PP_i (*right*). All dNTPs were supplied at 100 μM, except for dATP, whose concentration was 1 μM to avoid inhibition of the excision reaction due to the formation of a dead-end complex. Template/primer concentration was 30 nM. RTs were used at 72 nM and 24 nM concentrations (active sites), in rescue reactions carried out in the presence of ATP or PP_i, respectively. Represented values were obtained from at least three independent experiments. Rescue rates (k_{obs} values) are given in the supplemental Table S2.

bated in the presence of the inhibitor to generate a terminated 26-nucleotide primer. Then, unblocking and extension reactions were carried out by adding a mixture of dNTPs and a PP_i donor (ATP or PP_i). A mutant RT lacking Asp-67 and having the β3-β4 hairpin loop consensus sequence KKKSGRWR (*i.e.* mutant Δ67/T69G/K70R) showed relatively high ATP-dependent phosphorolytic activity on primers terminated with AZTMP (Fig. 1*B*). In contrast, WT (NL4–3) RT and mutant RTs Δ67, Δ69, and S68G/Δ69/K70G showed almost negligible activity. Similar results were obtained with primers terminated with d4TMP, although the efficiency of the reaction was reduced (Fig. 1*C*).

After incubating for 30 min under our assay conditions and in the presence of ATP, Δ67/T69G/K70R RT rescued 60% of the AZTMP-terminated primer, but less than 20% of the primer blocked with d4TMP (Fig. 1). A double mutant containing the deletion of codon 67 and K70R also showed detectable ATP-mediated excision activity on both types of hybrids, but its catalytic efficiency was reduced >2-fold in comparison with the Δ67/T69G/K70R RT (data not shown). In the presence of 200 μM PP_i all RTs were able to unblock and extend primers blocked with AZTMP or d4TMP, although efficiencies were lower for mutant RTs Δ67 and S68G/Δ69/K70G (rescue rates are given in the supplemental Table S2). Both mutants containing Δ69 produced a small but significant reduction of the ATP-mediated excision activity in comparison with the WT enzyme.

The effects of Δ67 and Δ69 on the ATP-dependent phosphorolytic activity were also tested in the presence of TAMs M41L and T215Y. The introduction of the Δ67 complex of mutations (Δ67/T69G/K70R) produced a 2-fold increase in the ATP-mediated excision activity on AZTMP- and d4TMP-terminated primers (Fig. 2). On the other hand, the Δ69 complex (*i.e.* S68G/Δ69/K70G) had an antagonistic effect on the ATP-mediated excision activity of M41L/T215Y RT. These effects were also observed with AZTMP-terminated primers in the presence of PP_i, although differences were less pronounced (Fig. 2*A*). In contrast, all tested enzymes showed similar rescue efficiencies on d4TMP-terminated primers in the presence of PP_i (Fig. 2*B*). These results were consistent with phenotypic susceptibility data showing that mutations S68G/Δ69/K70G resensitize

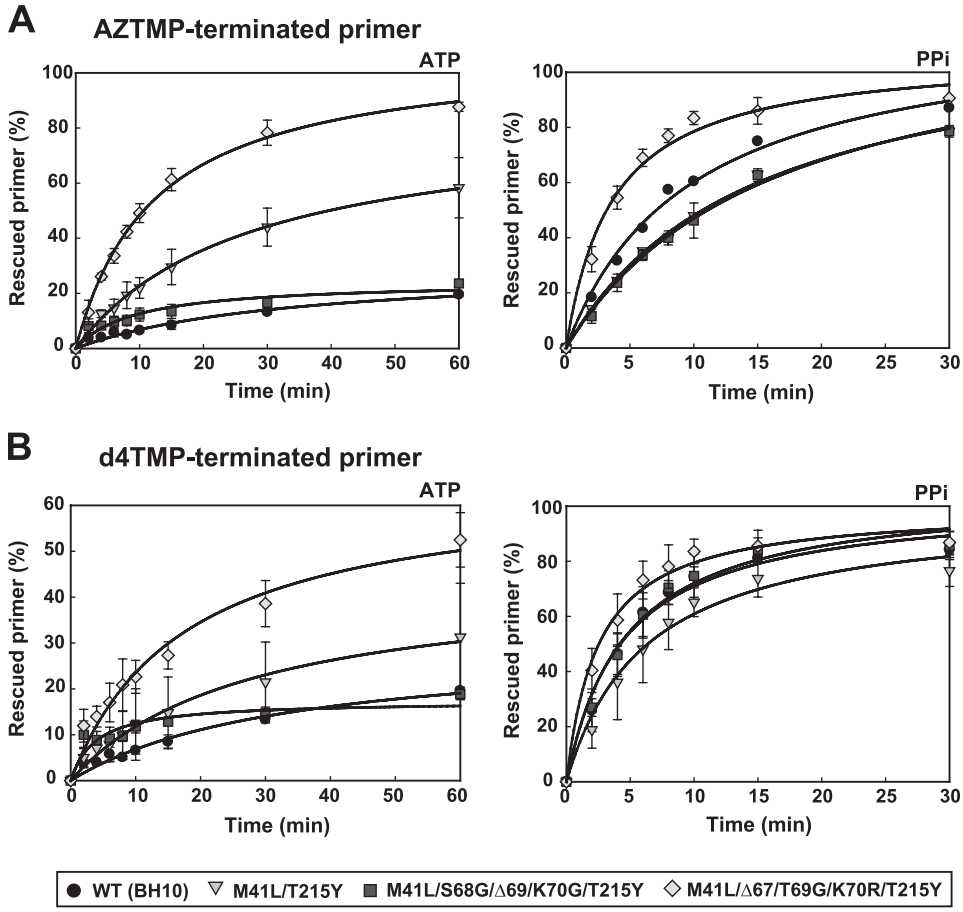

FIGURE 2. **Effect of amino acid substitutions S68G/Δ69/K70G and Δ67/T69G/K70R on rescue DNA polymerization reactions catalyzed by RTs carrying the thymidine analog mutations M41L and T215Y.** Time courses of reactions initiated from primers terminated with AZTMP (*A*) and d4TMP (*B*), and carried out in the presence of 3.2 mM ATP (*left*) or 200 μM PP_i (*right*). All dNTPs were supplied at 100 μM, except for dATP, whose concentration was 1 μM. The concentration of template/primer (D38/25PGA) was 30 nM. RTs were used at 72 nM and 24 nM concentrations (active sites), in rescue reactions carried out in the presence of ATP or PP_i, respectively. Represented values were obtained from at least three independent experiments. Rescue rates (k_{obs} values) are given in the supplemental Table S2.

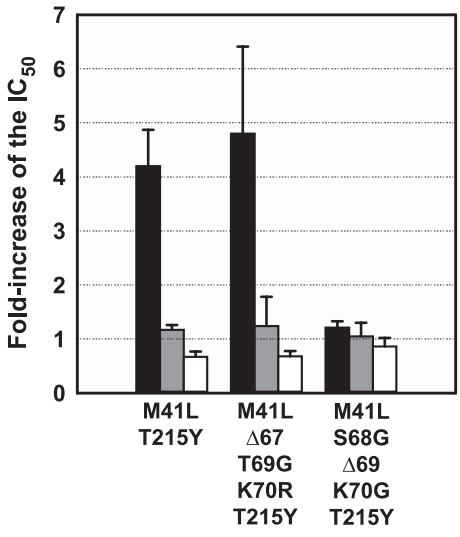

FIGURE 3. **Drug susceptibility measurements obtained with recombinant HIV-1 clones containing RTs M41L/Δ67/T69G/K70R/T215Y, M41L/S68G/Δ69/K70G/T215Y, and M41L/T215Y.** Represented values are the fold-increase in drug susceptibility of the indicated mutant viruses compared with those obtained with recombinant HIV containing the BH10 RT sequence. Drug susceptibility values for AZT, d4T, and ritonavir are shown using *black*, *gray*, and *white bars*, respectively.

HIV-1 to AZT, while Δ67/T69G/K70R produced a slight increase in AZT resistance (Fig. 3). The effects of the deletions in the viral susceptibility to d4T were relatively small due to inhibition of the excision reaction by the relatively high dNTP levels found in MT-4 cells used in phenotypic assays (38).

Structural Models for Ternary Complexes of Mutant RTs, Double-stranded DNA and dTTP—Structural models for mutant RTs Δ67/T69G/K70R and D67N/K70R were obtained by homology modeling based on the 1RTD coordinates (8), and refined by molecular dynamics. Simulations were followed over the 10-ns trajectory. The root-mean-square deviations (rmsd) corresponding to the backbone C_α atoms of the modeled ternary complexes remained below 2.3 Å during all the simulation time when compared with the crystal structure of the ternary complex containing the WT RT (supplemental Fig. S2*A*). At the end of the simulation, interactions at the catalytic site of the ternary complexes were similar to those observed in the crystal structure. In both models, mutations did not affect critical interactions required for maintaining the catalytic attack distance between the 3′-OH of the primer and the α phosphorous, and needed for the catalytic competence of the polymerase (supplemental Fig. S2*B*).

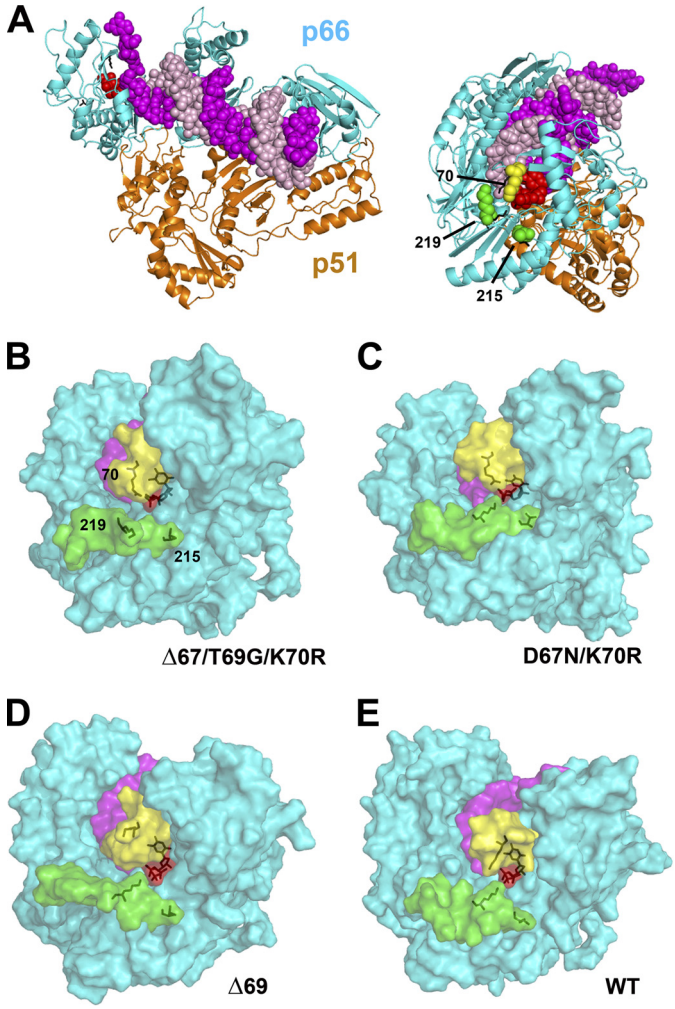

FIGURE 4. **Comparison of the structural models of mutant and WT HIV-1 RTs, complexed with dsDNA and an incoming dNTP.** *A*, crystal structure of the ternary complex of HIV-1 RT (*ribbon diagrams*), dsDNA (sphere model showing the template in *magenta* and the primer in *light pink*) and dTTP (*red spheres*). A side view of the complex showing the dNTP binding site and the location of Lys-70, Thr-215, and Lys-219 is shown on the right. *B–E*, views of the surface of the molecular models of mutant RTs Δ67/T69G/K70R (*B*), D67N/K70R (*C*), and Δ69 (*D*) and the WT enzyme (*E*), showing the location of β3-β4 hairpin loop residues 64–72 (*yellow*) and residues 215–227 (*green*). The dsDNA and the incoming dNTP (partially hidden by the color structures) are shown in *magenta* and *red*, respectively. *Stick representations* are use to indicate the location of the incoming dNTP and the side chains at positions 70, 215, and 219 (numbering as in the WT HIV-1 RT). All RTs (66-kDa subunits) were previously aligned and superimposed using PyMol, and are presented in the same orientation as the structure shown in *panel A* (*right*).

The largest differences between the modeled structures of Δ67/T69G/K70R and D67N/K70R RTs and the previously published molecular models of Δ69 RT (24) and WT RT (34) were observed at the β3-β4 hairpin loop (residues 64–72) and between β-strand 11a (residues 214–217) and β-strand 12 (residues 227–229) (Fig. 4). More specifically, the positions of the side chains of Lys/Arg-70 and Lys-219 were largely affected by deletions in the β3-β4 hairpin loop. During the last 3.5 ns of the simulation, the distances between the ζ carbon of Arg-70 and the γ phosphorous of the dNTP remained stable and below 4.5 Å in the models of Δ67/T69G/K70R and D67N/K70R RTs, and these distances were compatible with the establishment of hydrogen-bonding interactions between amido groups of Arg-70 and hydroxyl substituents of the γ phosphate of the incoming nucleotide (supplemental Fig. S3). However, in the model of WT HIV-1 RT/dsDNA/dTTP (Fig. 4*E*), the distance between the ϵ-amino group of Lys-70 and hydroxyl substituents of the γ phosphate of dTTP increased up to 4.2 Å, while in Δ69 RT, the distance was 13.7 Å. The side chain of Lys-219 was close to the γ phosphate of dTTP in the modeled structures of D67N/K70R, Δ69, and WT RTs (distances <3.5 Å), but away from the incoming dNTP in the Δ67/T69G/K70R RT (distance >8 Å). It should be noted that the salt bridge between the side chains of Asp-67 and Lys-219, present in the crystal structure of the ternary complex of HIV-1 RT, dsDNA and dTTP (supplemental Fig. S4) cannot be formed in the mutant RTs Δ67/T69G/K70R and D67N/K70R because of the loss of the acidic Asp residue.

Effects of the Amino Acid Substitution K219E on the Discrimination between dTTP and AZTTP by Deletion-containing RTs—Previous modeling studies carried out with the Δ69 RT (24) together with evidence based on amino acid sequence analysis suggested that substituting Glu or Gln for Lys-219 could have an effect on discrimination of AZTTP *versus* dTTP, or on the excision of thymidine analogues from terminated primers. The different conformations of β-strands 11a and 12 relative to the β3-β4 hairpin loop in deletion-containing RTs also support these proposals (Fig. 4). Pre-steady-state kinetic analysis of dTTP incorporation carried out with WT (NL4–3) and mutant RTs revealed minor differences between the WT enzyme and the mutant Δ67/T69G/K70R. However, RTs carrying the deletion at position 69 showed about 2-fold decreased catalytic efficiency (k_{pol}/K_d) of dTTP incorporation (Table 1). Introducing K219E had no effect on dTTP incorporation when Δ69 was present, but mutant Δ67/T69G/K70R/K219E showed higher efficiency of dTTP and AZTTP incorporation than the parental Δ67/T69G/K70R RT. These two enzymes showed over 2-fold higher selectivity for AZTTP *versus* dTTP in comparison with the WT RT and the Δ69-containing RTs. This was due to their higher affinity (*i.e.* lower K_d) for AZTTP. WT RT and the Δ69 derivatives showed K_d values for AZTTP in the range of 18.9–42.4 μM, higher than those previously reported for WT and Δ69 RTs (24). The introduction of K219E in RTs containing Δ69 or S68G/Δ69/K70G led to a small reduction of the selectivity of AZTTP *versus* dTTP.

Effects of K219E on the Excision Activity of Deletion-containing RTs—Rescue DNA polymerization assays using AZTMP- and d4TMP-terminated primers revealed only minor differences between Δ67/T69G/K70R/K219E and Δ67/T69G/K70R RTs in the presence of 3.2 mM ATP or 200 μM PP_i (Fig. 5). However, in the presence of 200 μM PP_i, rescue efficiencies in reactions catalyzed by mutant RTs Δ69/K219E and S68G/Δ69/K70G/K219E were lower than those obtained with Δ69 and S68G/Δ69/K70G RTs. These effects were observed with both AZTMP- and d4TMP-terminated primers. However, in the presence of 3.2 mM ATP, rescue efficiencies were very low and the effects of K219E on the excision reaction were almost undetectable. Previous studies carried out with a WT HIV-1 RT showed that in the presence of high concentrations of GTP (*i.e.* above 3 mM), NRTI excision rates were about 4-fold higher than in the presence of 3.2 mM ATP (39). Therefore, we tested

TABLE 1

Pre-steady-state kinetic constants for the incorporation of dTTP and AZTTP into heteropolymeric template/primer by wild-type and mutant RTs

The template/primer 31T/21P was used as the substrate. Data shown are the mean values ± S.D. Each of the assays was performed independently at least three times. Inter-assay variability was below 20%. All determinations were carried out under single turnover conditions.

RT	Nucleotide	k_{pol}	K_d	k_{pol}/K_d	Selectivity[a]
		s^{-1}	μM	$\mu M^{-1}s^{-1}$	
WT (NL4-3)	dTTP[b]	17.4 ± 2.0	7.1 ± 2.5	2.47 ± 0.93	0.47 ± 0.20
	AZTTP	22.1 ± 1.6	18.9 ± 3.6	1.17 ± 0.24	
Δ67/T69G/K70R	dTTP	22.4 ± 1.4	13.2 ± 2.7	1.70 ± 0.36	1.15 ± 0.32 (2.4)
	AZTTP	8.6 ± 0.3	4.4 ± 0.8	1.95 ± 0.36	
Δ67/T69G/K70R/K219E	dTTP	19.9 ± 0.8	5.5 ± 1.1	3.62 ± 0.74	1.00 ± 0.31 (2.1)
	AZTTP	9.4 ± 0.4	2.6 ± 0.6	3.61 ± 0.80	
Δ69	dTTP[b]	12.3 ± 1.0	14.8 ± 3.0	0.83 ± 0.18	0.55 ± 0.17 (1.2)
	AZTTP	14.0 ± 1.1	30.6 ± 6.2	0.46 ± 0.10	
Δ69/K219E	dTTP	12.4 ± 1.3	14.8 ± 5.1	0.83 ± 0.29	0.28 ± 0.13 (0.6)
	AZTTP	9.8 ± 1.0	42.4 ± 11.9	0.23 ± 0.07	
S68G/Δ69/K70G	dTTP	11.1 ± 0.5	10.3 ± 1.4	1.08 ± 0.15	0.42 ± 0.11 (0.9)
	AZTTP	16.4 ± 1.6	35.4 ± 7.3	0.46 ± 0.10	
S68G/Δ69/K70G/K219E	dTTP	10.8 ± 0.9	11.0 ± 3.2	0.97 ± 0.30	0.30 ± 0.14 (0.6)
	AZTTP	9.7 ± 1.1	32.8 ± 11.0	0.29 ± 0.10	

[a] The selectivity is the ratio of $[k_{pol}/K_d$ (AZTTP)$]/[k_{pol}/K_d$ (dTTP)]. Resistance (shown between parentheses) was calculated as the selectivity value obtained with each mutant enzyme divided by the selectivity obtained with the WT RT.

[b] Data were taken from Kisic *et al.* (24).

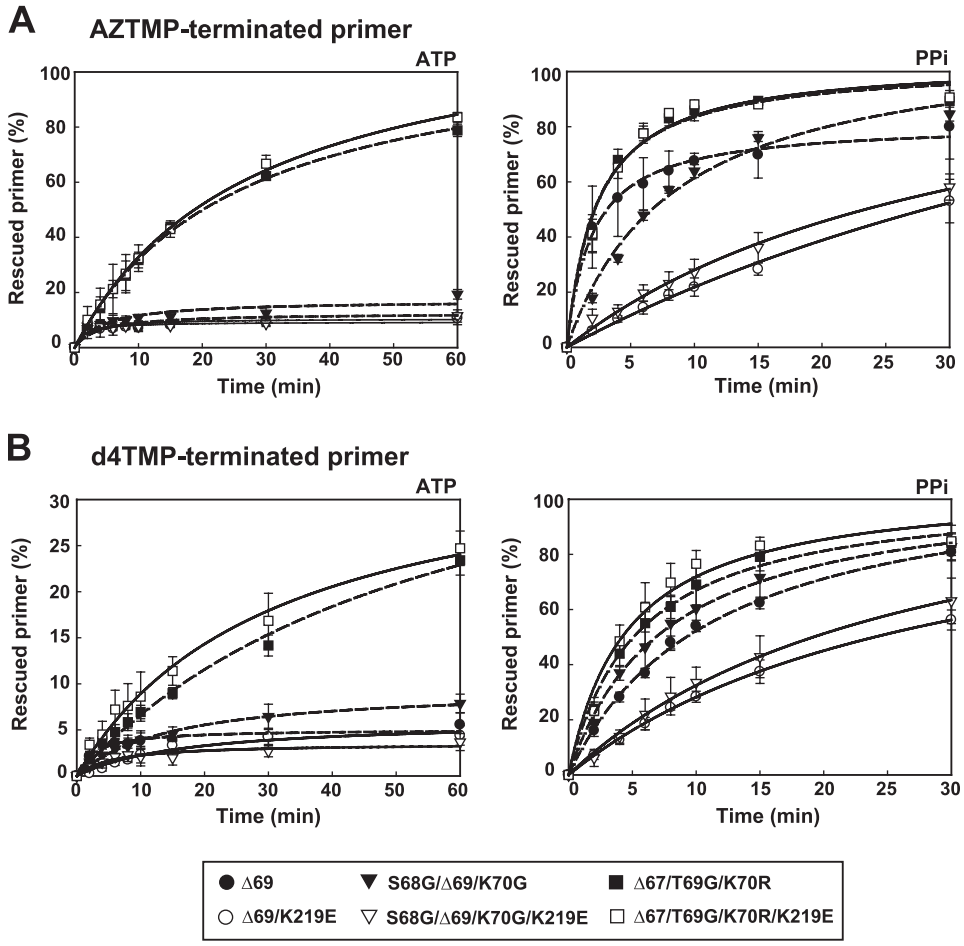

FIGURE 5. **Effects of amino acid substitution K219E on rescue DNA polymerization reactions catalyzed by RTs carrying deletions in the β3-β4 hairpin loop.** Time courses of reactions initiated from primers terminated with AZTMP (*A*) and d4TMP (*B*), and carried out in the presence of 3.2 mM ATP (*left*) or 200 μM PP_i (*right*). All dNTPs were supplied at 100 μM, except for dATP, whose concentration was 1 μM. The concentration of the template/primer (D38/25PGA) was 30 nM. RTs were used at 72 and 24 nM concentrations (active sites), in rescue reactions carried out in the presence of ATP or PP_i, respectively. Represented values were obtained from at least three independent experiments. Rescue rates (k_{obs} values) are given in the supplemental Table S2.

whether the effects of K219E on NRTI excision could be detected in the presence of GTP. As shown in Fig. 6, unblocking and extension efficiencies of AZTMP-terminated primers catalyzed by Δ69 and S68G/Δ69/K70G RTs were significantly reduced after replacing Glu for Lys-219.

Susceptibility to Thymidine Analogues of Recombinant HIV-1—Recombinant HIV-1 clones containing RTs bearing mutations Δ67/T69G/K70R, Δ69, or S68G/Δ69/K70G with or without K219E were assayed to establish the level of resistance to thymidine analogues in comparison with the WT (NL4–3) RT. As

shown in Table 2, both Δ67/T69G/K70R and Δ67/T69G/K70R/K219E conferred >8-fold increased AZT resistance and showed reduced susceptibility to d4T compared with the WT virus (1.5-fold increase of the IC_{50}). All HIV-1 variants that contained RTs lacking Thr-69 were susceptible to AZT, d4T, and foscarnet. AZT hypersusceptibility was observed for recombinant HIV-1 bearing RT mutations Δ69, Δ69/K219E, and S68G/Δ69/K70G. However, in the presence of β3-β4 hairpin loop deletions, K219E had a relatively small effect on thymidine analog resistance as determined in phenotypic assays, using recombinant HIV-1 variants.

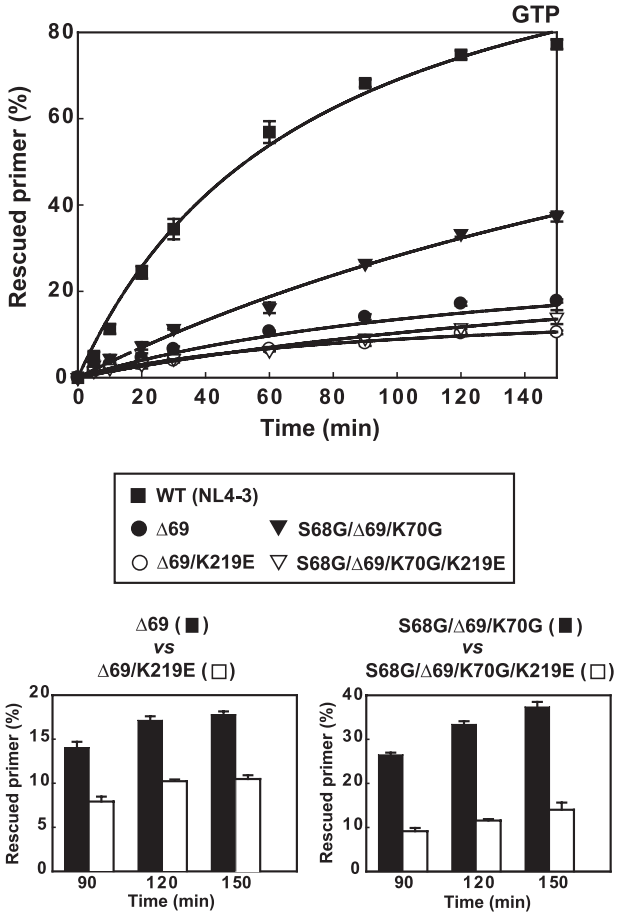

FIGURE 6. **Effect of amino acid substitution K219E on GTP-dependent excision efficiencies with primers terminated with AZTMP.** Rescue DNA polymerization assays were carried out in the presence of 9.6 mM GTP. All dNTPs were supplied at 100 μM, except for dATP, whose concentration was 1 μM. Template primer (D38/25PGA) and active RT concentrations in these assays were 30 nM and 72 nM, respectively. The *lower panels* show direct comparisons between rescue efficiencies of RTs with and without K219E, at selected times. Represented values were obtained from at least three independent experiments.

DISCUSSION

A significant number of mutations conferring resistance to NRTIs has been demonstrated to appear in the β3-β4 hairpin loop (residues 64–72) of HIV-1 RT (1, 5). Hydrogen bonds between the side chains of Lys-65 and Arg-72 and the triphosphate moiety of the incoming dNTP are required for the stabilization of the dNTP/Mg^{2+} complex within the nucleotide binding site of the RT (8). Amino acid sequences around the β3-β4 region of the RT show remarkable variability, with Δ69/Δ70 deletions appearing frequently in combination with the Q151M complex (21, 23, 40, 41), and Δ67 in isolates containing TAMs (22, 26, 40). We found that more than 90% of the HIV-1 *pol* sequences bearing a deletion at codon 67 contained additional mutations at neighboring residues (usually T69G and K70R).

Our study demonstrates that β3-β4 hairpin loop deletions have distinct effects on thymidine analog excision, and therefore introduce functional constraints on the evolutionary pathways leading to multidrug resistance. Thus, Δ69 alone or associated with S68G and K70G decrease ATP-mediated NRTI excision on primers terminated with both AZT or d4T in different sequence contexts. This effect is consistent with the reported AZT hypersusceptibility observed in phenotypic assays with HIV-1 clones bearing Δ69/Δ70 deletions (23, 24, 41), as well as with the antagonistic effects of Δ69 and M41L/T215Y found in our AZT susceptibility assays carried out with recombinant HIV-1. Interestingly, by itself, the Δ67 complex (*i.e.* Δ67/T69G/K70R) confers significant ATP-dependent phosphorolytic activity on primers terminated with AZT, and to a lesser extent with d4T. These results were consistent with the >8-fold decreased susceptibility to AZT observed in phenotypic assays with HIV-1 containing the Δ67/T69G/K70R RT.

The deletion of codon 67 had a minor effect on excision, in agreement with previous studies showing that neither Δ67 alone nor the combination Δ67/T69G confer significant levels of AZT resistance in phenotypic assays (21, 25, 26). Only K70R appears to have a modest effect on AZT resistance (2–4-fold increase of the IC_{50} for the inhibitor) (42, 43). A study of the clinical evolution of a patient infected with an HIV-1 isolate bearing the 67 deletion has revealed its emergence after the accumulation of several TAMs including K70R and the previ-

TABLE 2

Susceptibility of HIV-1 constructs to AZT, d4T, and Foscarnet

The IC_{50} values represent the mean ± S.D. of at least three tests, with each one performed six times. The fold increase in IC_{50} relative to the wild-type HXB2 virus control carrying the RT sequence of NL4–3 is shown in parenthesis.

RTs	IC_{50}		
	AZT	d4T	Foscarnet
	nM	nM	nM
WT (NL4-3)	5.4 ± 1.1	274.6 ± 44.5	44637 ± 10687
Δ67/T69G/K70R	47.0 ± 6.3 (8.7)	451.8 ± 60.3 (1.6)	119068 ± 16753 (2.7)
Δ67/T69G/K70R/K219E	57.5 ± 24.3 (10.6)	390.5 ± 109.5 (1.4)	27772 ± 4942 (0.6)
Δ69	2.5 ± 0.7 (0.4)	231.8 ± 103.9 (0.8)	31133 ± 5428 (0.7)
Δ69/K219E	2.5 ± 0.4 (0.4)	294.0 ± 87.8 (1.1)	21260 ± 1357 (0.5)
S68G/Δ69/K70G	3.7 ± 1.1 (0.7)	295.1 ± 83.7 (1.1)	33138 ± 6976 (0.7)
S68G/Δ69/K70G/K219E	8.0 ± 1.3 (1.5)	394.9 ± 111.0 (1.4)	40265 ± 8148 (0.9)

ous selection of D67N (26). Our data support the functional equivalence of the Δ67/T69G/K70R complex and the double mutation D67N/K70R. Previously reported phenotypic data showed that D67N/K70R confers 4.6-fold and 1.4-fold increased resistance to AZT and d4T, respectively (44). These values are similar to those found in our study for HIV-1 bearing the Δ67/T69G/K70R RT. The equivalence is also consistent with the remarkable ATP-mediated excision activity of both mutant RTs on primers terminated with NRTIs (9; this work). In addition, as reported for D67N/K70R (9), the Δ67/T69G/K70R complex enhances the ATP-dependent phosphorolytic activity of RTs bearing TAMs such as M41L and T215Y.

Homology modeling and molecular dynamics studies show large differences in the conformation of the β3-β4 hairpin loop among the predicted structures of WT, Δ69, and Δ67/T69G/K70R RTs, in complex with a dideoxyguanosine-terminated primer-template (dsDNA) and dTTP. Major differences among RTs affect the location and interactions involving the side chains of Lys/Arg-70 and Lys-219. In the crystal structure of the ternary complex of WT HIV-1 RT/dsDNA/dTTP (8), the two lysine residues are located in the vicinity of the γ phosphate of the incoming dNTP, with the side chain of Lys-219 interacting with the side chain of Asp-67. This interaction is lost in molecular dynamics simulations obtained after introducing a 3′-OH group at the blocked primer (34), while the ϵNH_2 group of Lys-219 moves to interact with the γ phosphate of dTTP. Based on modeling studies, Boyer *et al.* (11) have proposed that during the excision reaction, the γ and β phosphates of the incoming dNTP in the ternary complex would occupy positions similar to those expected for the β and γ phosphates of ATP in the excision reaction. The recently published structure of an AZT-resistant RT (M41L/D67N/K70R/T215Y/K219Q) bound to dsDNA and the product of the ATP-mediated excision of AZT monophosphate from the 3′-end of the primer (*i.e.* AZT adenosine dinucleotide tetraphosphate, AZTppppA) (28) is consistent with this hypothesis (supplemental Fig. S4). Although Arg-70 may not be required for ATP binding if Tyr-215 is present, hydrogen bonds between the side chains of residues 65, 70, and 219 play a pivotal role in the stabilization of AZTppppA in this structure and are likely to participate in the excision reaction by placing the PP_i moiety of ATP in the proper orientation for nucleophilic attack.

Our modeling studies show that the large differences in the conformation of the β3-β4 hairpin loop in WT and mutant RTs do have a major impact on the position of Lys/Arg-70. Arg-70 seems to interact with the incoming dNTP in both Δ67/T69G/K70R and D67N/K70R RTs, suggesting that it could also interact with the β phosphate of ATP during the excision reaction. In contrast, the side chain of Lys-70 in the Δ69 RT is located away from the γ phosphate of dTTP, suggesting the loss of its putative function in PP_i donor binding, and in agreement with the lower excision activity of Δ69-containing RTs relative to the WT enzyme.

The loss of interactions between the PP_i donor and the mutant RT could also explain the further reduced excision activity of the Δ69/K219E and S68G/Δ69/K70G/K219E RTs, observed in the presence of either PP_i or GTP. Substituting Glu for Lys-219 would result in the loss of potential hydrogen bonds and ionic interactions between the enzyme and the incoming dNTP in all RTs, although the presence of a basic residue in its vicinity (*e.g.* Lys/Arg-70) could mitigate these effects. This basic environment would be lost in Δ69/K219E and S68G/Δ69/K70G/K219E RTs. Interestingly, adding K219E to the Δ67/T69G/K70R complex has no effect on excision, although it increases the catalytic efficiency of the RT in dTTP and AZTTP incorporation assays. The lower excision activity of Δ69/K219E and S68G/Δ69/K70G/K219E RTs compared with Δ69 and S68G/Δ69/K70G RTs does not increase HIV-1 susceptibility to AZT in phenotypic assays. Substituting Glu for Lys-219 in RTs bearing the 69 deletion contributes to AZT resistance by reducing AZTTP incorporation efficiency, and thereby antagonizing its potential effects on excision that could lead to enhanced AZT hypersusceptibility.

Taken together, our results are also consistent with clinical data showing that HIV-1 develops TAMs by one of two distinct pathways, defined as the TAM1 pathway (including mutations M41L, L210W, and T215Y) or the TAM2 pathway (involving mutations D67N, K70R, K219E/Q, and sometimes T215F) (45–47). TAM2 clustering studies revealed that K219E and K219Q are more likely to develop if there was previous selection of K70R (47). In this context, Δ67/T69G/K70R/K219E emerges as a novel cluster of TAM2 mutations that confer resistance to thymidine analogues through an excision-mediated mechanism.

Acknowledgment—We thank Luis Gosálbez for technical assistance in enzyme purification.

REFERENCES

1. Sarafianos, S. G., Marchand, B., Das, K., Himmel, D. M., Parniak, M. A., Hughes, S. H., and Arnold, E. (2009) *J. Mol. Biol.* **385,** 693–713
2. Herschhorn, A., and Hizi, A. (2010) *Cell. Mol. Life Sci.* **67,** 2717–2747
3. De Clercq, E. (2010) *Curr. Opin. Pharmacol.* **10,** 507–515
4. Menéndez-Arias, L. (2010) *Antiviral Res.* **85,** 210–231
5. Menéndez-Arias, L. (2008) *Virus Res.* **134,** 124–146
6. Sarafianos, S. G., Das, K., Clark, Jr. A. D., Ding, J., Boyer, P. L., Hughes, S. H., and Arnold, E. (1999) *Proc. Natl. Acad. Sci. U.S.A.* **96,** 10027–10032
7. Deval, J., Selmi, B., Boretto, J., Egloff, M. P., Guerreiro, C., Sarfati, S., and Canard, B. (2002) *J. Biol. Chem.* **277,** 42097–42104
8. Huang, H., Chopra, R., Verdine, G. L., and Harrison, S. C. (1998) *Science* **282,** 1669–1675
9. Meyer, P. R., Matsuura, S. E., Mian, A. M., So, A. G., and Scott, W. A. (1999) *Mol. Cell* **4,** 35–43
10. Meyer, P. R., Matsuura, S. E., Schinazi, R. F., So, A. G., and Scott, W. A. (2000) *Antimicrob. Agents Chemother.* **44,** 3465–3472
11. Boyer, P. L., Sarafianos, S. G., Arnold, E., and Hughes, S. H. (2001) *J. Virol.* **75,** 4832–4842
12. Naeger, L. K., Margot, N. A., and Miller, M. D. (2001) *Antivir. Ther.* **6,** 115–126
13. Mas, A., Vázquez-Álvarez, B. M., Domingo, E., and Menéndez-Arias, L. (2002) *J. Mol. Biol.* **323,** 181–197
14. Larder, B. A., Darby, G., and Richman, D. D. (1989). *Science* **243,** 1731–1734
15. Larder, B. A., Coates, K. E., and Kemp, S. D. (1991) *J. Virol.* **65,** 5232–5236
16. Kellam, P., Boucher, C. A., and Larder, B. A. (1992) *Proc. Natl. Acad. Sci. U.S.A.* **89,** 1934–1938
17. Harrigan, P. R., Kinghorn, I., Bloor, S., Kemp, S. D., Nájera, I., Kohli, A., and Larder, B. A. (1996) *J. Virol.* **70,** 5930–5934
18. Hooker, D. J., Tachedjian, G., Solomon, A. E., Gurusinghe, A. D., Land, S., Birch, C., Anderson, J. L., Roy, B. M., Arnold, E., and Deacon, N. J. (1996)

J. Virol. **70,** 8010–8018
19. Menéndez-Arias, L., Matamoros, T., and Cases-González, C. E. (2006) *Curr. Pharm. Des.* **12,** 1811–1825
20. Eggink, D., Huigen, M. C., Boucher, C. A., Götte, M., and Nijhuis, M. (2007) *Antiviral Res.* **75,** 93–103
21. Winters, M. A., Coolley, K. L., Cheng, P., Girard, Y. A., Hamdan, H., Kovari, L. C., and Merigan, T. C. (2000) *J. Virol.* **74,** 10707–10713
22. Masquelier, B., Race, E., Tamalet, C., Descamps, D., Izopet, J., Buffet-Janvresse, C., Ruffault, A., Mohammed, A. S., Cottalorda, J., Schmuck, A., Calvez, V., Dam, E., Fleury, H., Brun-Vézinet, F., and the ANRS AC11 Resistance Study Group (2001) *Antimicrob. Agents Chemother.* **45,** 1836–1842
23. Villena, C., Prado, J. G., Puertas, M. C., Martínez, M. A., Clotet, B., Ruiz, L., Parkin, N. T., Menéndez-Arias, L., and Martinez-Picado, J. (2007) *J. Virol.* **81,** 4713–4721
24. Kisic, M., Mendieta, J., Puertas, M. C., Parera, M., Martínez, M. A., Martinez-Picado, J., and Menéndez-Arias, L. (2008) *J. Mol. Biol.* **382,** 327–341
25. Imamichi, T., Murphy, M. A., Imamichi, H., and Lane, H. C. (2001) *J. Virol.* **75,** 3988–3992
26. Imamichi, T., Sinha, T., Imamichi, H., Zhang, Y. M., Metcalf, J. A., Falloon, J., and Lane, H. C. (2000) *J. Virol.* **74,** 1023–1028
27. Boyer, P. L., Imamichi, T., Sarafianos, S. G., Arnold, E., and Hughes, S. H. (2004) *J. Virol.* **78,** 9987–9997
28. Tu, X., Das, K., Han, Q., Bauman, J. D., Clark Jr., A. D., Hou, X., Frenkel, Y. V., Gaffney, B. L., Jones, R. A., Boyer, P. L., Hughes, S. H., Sarafianos, S. G., and Arnold, E. (2010) *Nature Struct. Mol. Biol.* **17,** 1202–1209
29. Betancor, G., Puertas, M. C., Nevot, M., Garriga, C., Martínez, M. A., Martinez-Picado, J., and Menéndez-Arias, L. (2010) *Antimicrob. Agents Chemother.* **54,** 4799–4811
30. Boretto, J., Longhi, S., Navarro, J. M., Selmi, B., Sire, J., and Canard, B. (2001) *Anal. Biochem.* **292,** 139–147
31. Matamoros, T., Deval, J., Guerreiro, C., Mulard, L., Canard, B., and Menéndez-Arias, L. (2005) *J. Mol. Biol.* **349,** 451–463
32. Kati, W. M., Johnson, K. A., Jerva, L. F., and Anderson, K. S. (1992) *J. Biol. Chem.* **267,** 25988–25997
33. Martín-Hernández, A. M., Gutiérrez-Rivas, M., Domingo, E., and Menéndez-Arias, L. (1997) *Nucleic Acids Res.* **25,** 1383–1389
34. Mendieta, J., Cases-González, C. E., Matamoros, T., Ramírez, G., and Menéndez-Arias, L. (2008) *Proteins* **71,** 565–574
35. Matamoros, T., Nevot, M., Martínez, M. A., and Menéndez-Arias, L. (2009) *J. Biol. Chem.* **284,** 32792–32802
36. Cases-González, C. E., Franco, S., Martínez, M. A., and Menéndez-Arias, L. (2007) *J. Mol. Biol.* **365,** 298–309
37. Kellam, P., and Larder, B. A. (1994) *Antimicrob. Agents Chemother.* **38,** 23–30
38. Smith, A. J., and Scott, W. A. (2006) *Curr. Pharm. Des.* **12,** 1827–1841
39. Meyer, P. R., Matsuura, S. E., So, A. G., and Scott, W. A. (1998) *Proc. Natl. Acad. Sci. U.S.A.* **95,** 13471–13476
40. Ross, L., Johnson, M., Ferris, R. G., Short, S. A., Boone, L. R., Melby, T. E., Lanier, R., Shaefer, M., and St. Clair, M. (2000) *J. Hum. Virol.* **3,** 144–149
41. Hu, Z., Hatano, H., Hammond, S. P., Smith, D., Wild, M., Gupta, S., Whitcomb, J., Kalayjian, R. C., Gripshover, B., and Kuritzkes, D. R. (2007) *J. Acquir. Immune Defic Syndr.* **45,** 494–500
42. Lacey, S. F., and Larder, B. A. (1994) *J. Virol.* **68,** 3421–3424
43. Ross, L., Parkin, N., Chappey, C., Fisher, R., St. Clair, M. S., Bates, M., Tisdale, M., and Lanier, E. R. (2004) *AIDS* **18,** 1691–1696
44. Brehm, J. H., Koontz, D., Meteer, J. D., Pathak, V., Sluis-Cremer, N., and Mellors, J. W. (2007) *J. Virol.* **81,** 7852–7859
45. Yahi, N., Tamalet, C., Tourrès, C., Tivoli, N., Ariasi, F., Volot, F., Gastaut, J. A., Gallais, H., Moreau, J., and Fantini, J. (1999) *J. Clin. Microbiol.* **37,** 4099–4106
46. Hanna, G. J., Johnson, V. A., Kuritzkes, D. R., Richman, D. D., Brown, A. J., Savara, A. V., Hazelwood, J. D., and D'Aquila, R. T. (2000) *J. Infect. Dis.* **181,** 904–911
47. Cozzi-Lepri, A., Ruiz, L., Loveday, C., Phillips, A. N., Clotet, B., Reiss, P., Ledergerber, B., Holkmann, C., Staszewski, S., and Lundgren, J. D. for the EuroSIDA Study Group (2005) *Antivir. Ther.* **10,** 791–802

SUPPLEMENTARY TABLE S1
Templates and synthetic oligonucleotides used in site-directed mutagenesis reactions

Insert in the p66RTB plasmid	Obtained RTs	Mutagenic primers [a]
WT (NL4-3) RT	Δ67/T69G/K70R	5' CCAGTATTTGCCATAAAGAAAAAAAGTGGTAGATGGAGAAAATTAGTA 3' 3' GGTCATAAACGGTATTTCTTTTTTTCACCATCTACCTCTTTTAATCAT 5'
M41L/T215Y (BH10) RT	M41L/Δ67/T69G/K70R/T215Y	
Δ69 (NL4-3) RT	S68G/Δ69/K70G	5' GCCATAAAGAAAAAAGACGGTGGATGGAGAAAATTAGTAG 3' 3' CGGTATTTCTTTTTTCTGCCTCCTACCTCTTTTAATCATC 5'
M41L/T215Y (BH10) RT	M41L/S68G/Δ69/K70G/T215Y	
Δ67/T69G/K70R (NL4-3) RT	Δ67	5' CCAGTATTTGCCATAAAGAAAAAAAGTACTAAATGGAGAAAATTAGTAG 3' 3' GGTCATAAACGGTATTTCTTTTTTTCATGATTTACCTCTTTTAATCATC 5'
Δ69 (NL4-3) RT	Δ69/K219E	5' GATTTACCACACCAGACGAAAAACATCAGAAAGAAC 3' 3' CTAAATGGTGTGGTCTGCTTTTTGTAGTCTTTCTTG 5'
Δ67/T69G/K70R (NL4-3) RT	Δ67/T69G/K70R/K219E	
S68G/Δ69/K70G (NL4-3) RT	S68G/Δ69/K70G/K219E	

[a] Underlined nucleotides correspond to mutations introduced in the RT coding region.

SUPPLEMENTARY TABLE S2
Rescue rates of AZTMP- and d4TMP-terminated primers in reactions catalyzed by wild-type and mutant RTs [a]

		AZTMP-teminated primers k_{obs} (min^{-1})		d4TMP-terminated primers k_{obs} (min^{-1})	
	RTs	ATP	PPi	ATP	PPi
Figure 1	WT (NL4-3)	*0.0124 ± 0.0003*	0.285 ± 0.006	*0.0048 ± 0.0010*	0.275 ± 0.011
	Δ67	*0.0115 ± 0.0007*	0.119 ± 0.003	*0.0039 ± 0.0004*	0.119 ± 0.006
	Δ69	*<0.0035*	0.368 ± 0.061	*<0.003*	0.101 ± 0.005
	S68G/Δ69/K70G	*0.0061 ± 0.0005*	0.128 ± 0.006	*<0.004*	0.135 ± 0.005
	Δ67/T69G/K70R	0.0482 ± 0.0011	0.327 ± 0.013	*0.0123 ± 0.0008*	0.172 ± 0.006
Figure 2	WT (BH10)	*0.0093 ± 0.0005*	0.114 ± 0.005	*<0.0035*	0.201 ± 0.007
	M41L/T215Y	0.0451 ± 0.0032	0.084 ± 0.004	*0.0148 ± 0.0011*	0.159 ± 0.009
	M41L/S68G/Δ69/K70G/T215Y	*0.0088 ± 0.0006*	0.078 ± 0.004	*0.0057 ± 0.0006*	0.194 ± 0.006
	M41L/Δ67/T69G/K70R/T215Y	0.0823 ± 0.0019	0.233 ± 0.007	*0.0229 ± 0.0020*	0.298 ± 0.009
Figure 5	Δ69/K219E	ND	0.024 ± 0.005	*<0.003*	0.050 ± 0.002
	S68G/Δ69/K70G/K219E	*<0.003*	0.044 ± 0.007	*<0.003*	0.053 ± 0.004
	Δ67/T69G/K70R/K219E	0.0452 ± 0.0015	0.316 ± 0.001	*0.0127 ± 0.0013*	0.197 ± 0.012

[a] Rescue rates (k_{obs} values) were obtained after fitting the data to a single exponential decay, [P] = A x [1 – exp(–k_{obs} x t)]. A linear regression was used to fit the data when rescue efficiencies were low (k_{obs} values shown in italics). In those cases we assumed that the amount of active RT was identical to the template-primer concentration used in the assay (*i.e.* 30 nM). ND stands for non-detectable rescue. Data shown are the mean values ± standard deviation, obtained from at least three independent experiments.

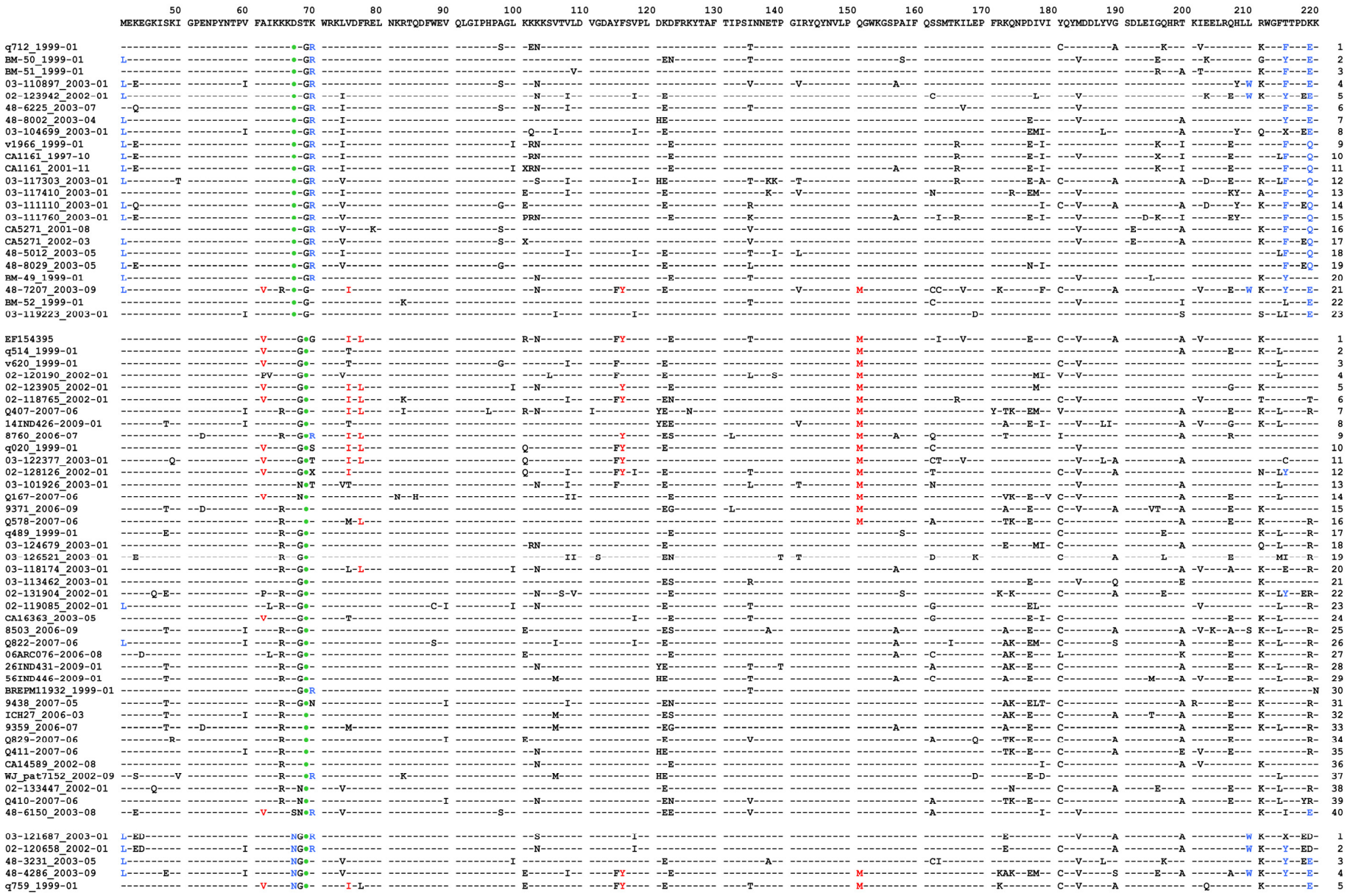

Supplementary Figure S1. Amino acid sequence alignments of the polymerase domain (residues 41-220) of HIV-1 RTs containing one-amino-acid deletions in the β3-β4 hairpin loop. Sequences were collected from Stanford HIV Drug Resistance Database (http://hivdb.stanford.edu) and classified into three major groups based on sequence conservation at the hairpin loop and accompanying drug resistance mutations. One-amino-acid deletions are represented by green dots. TAMs are indicated in blue and mutations of the Q151M complex in red.

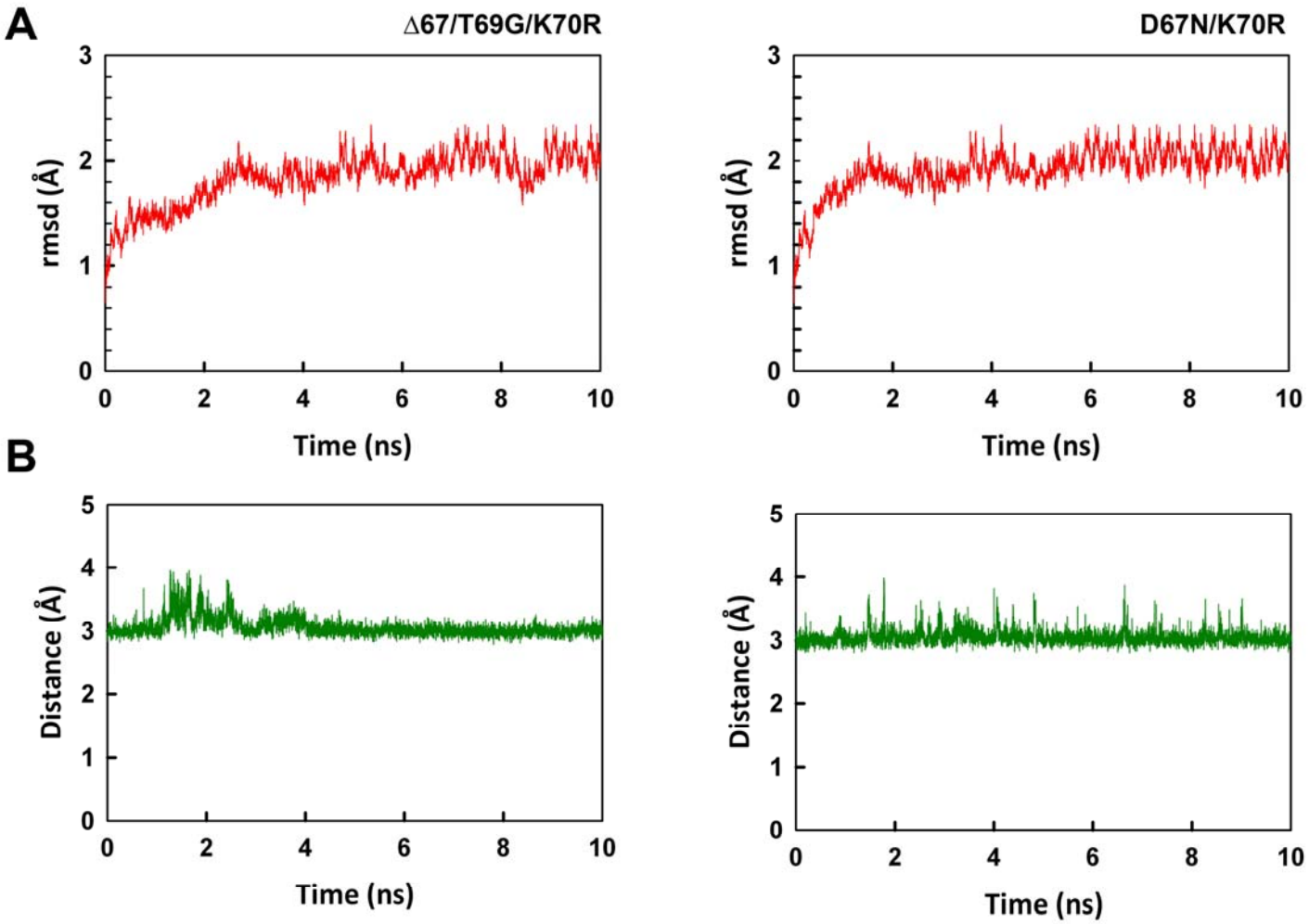

Supplementary Figure S2. Conformational changes in the ternary complexes containing HIV-1 RTs Δ67/T69G/K70R and D67N/K70R occurring along the simulation time. (A) Evolution of the rmsd of the Cα atoms of the 66-kDa subunit of the RT (residues 1-389) (red). (B) Evolution of the interatomic distance between the 3´ oxygen of the primer and the α phosphorous of the incoming dNTP (green) during molecular dynamics simulation.

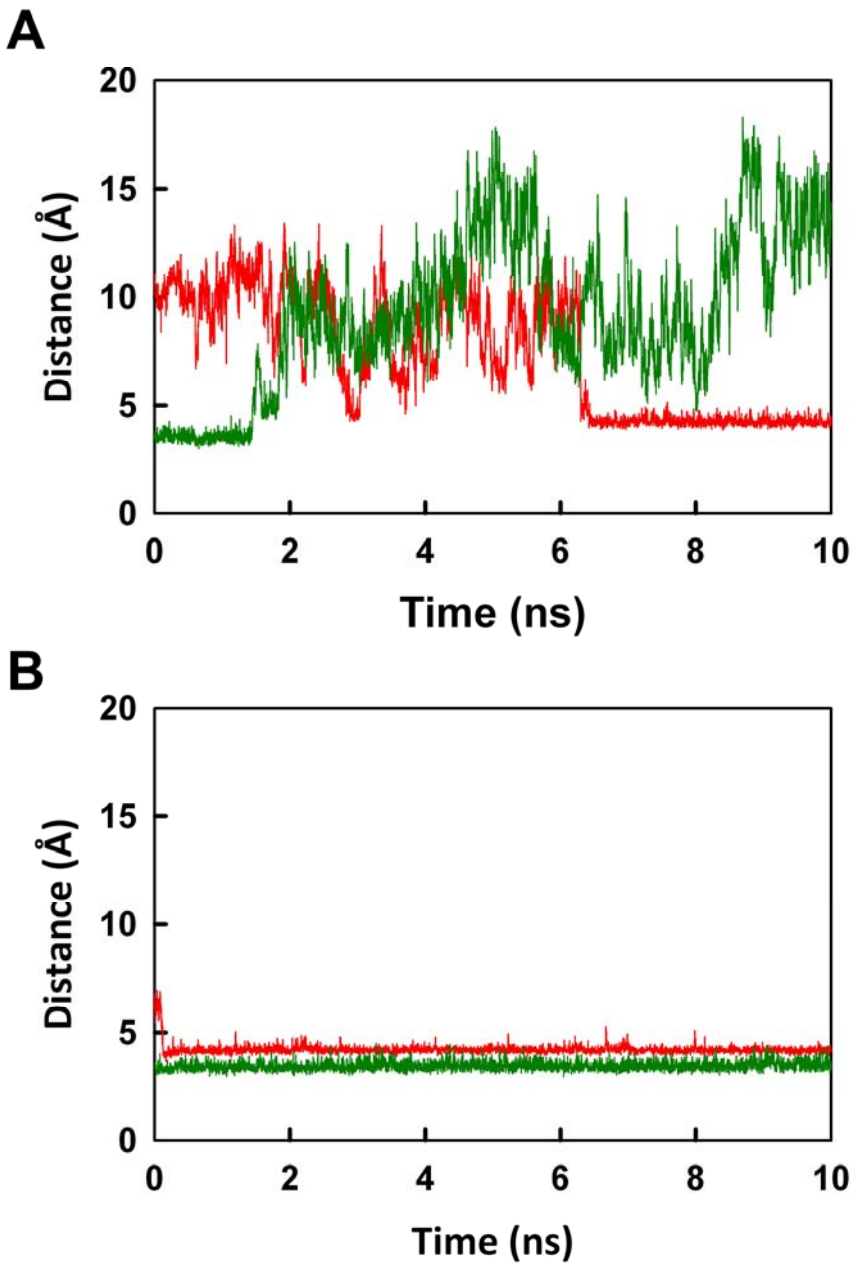

Supplementary Figure S3. Evolution of the inter-atomic distances between the ζ carbon of Arg70 and the γ phosphorous of the incoming dNTP (red) and between the ζ nitrogen of Lys219 and the γ phosphorous of the incoming dNTP (green), in ternary complexes of HIV-1 RTs Δ67/T69G/K70R (A) and D67N/K70R (B).

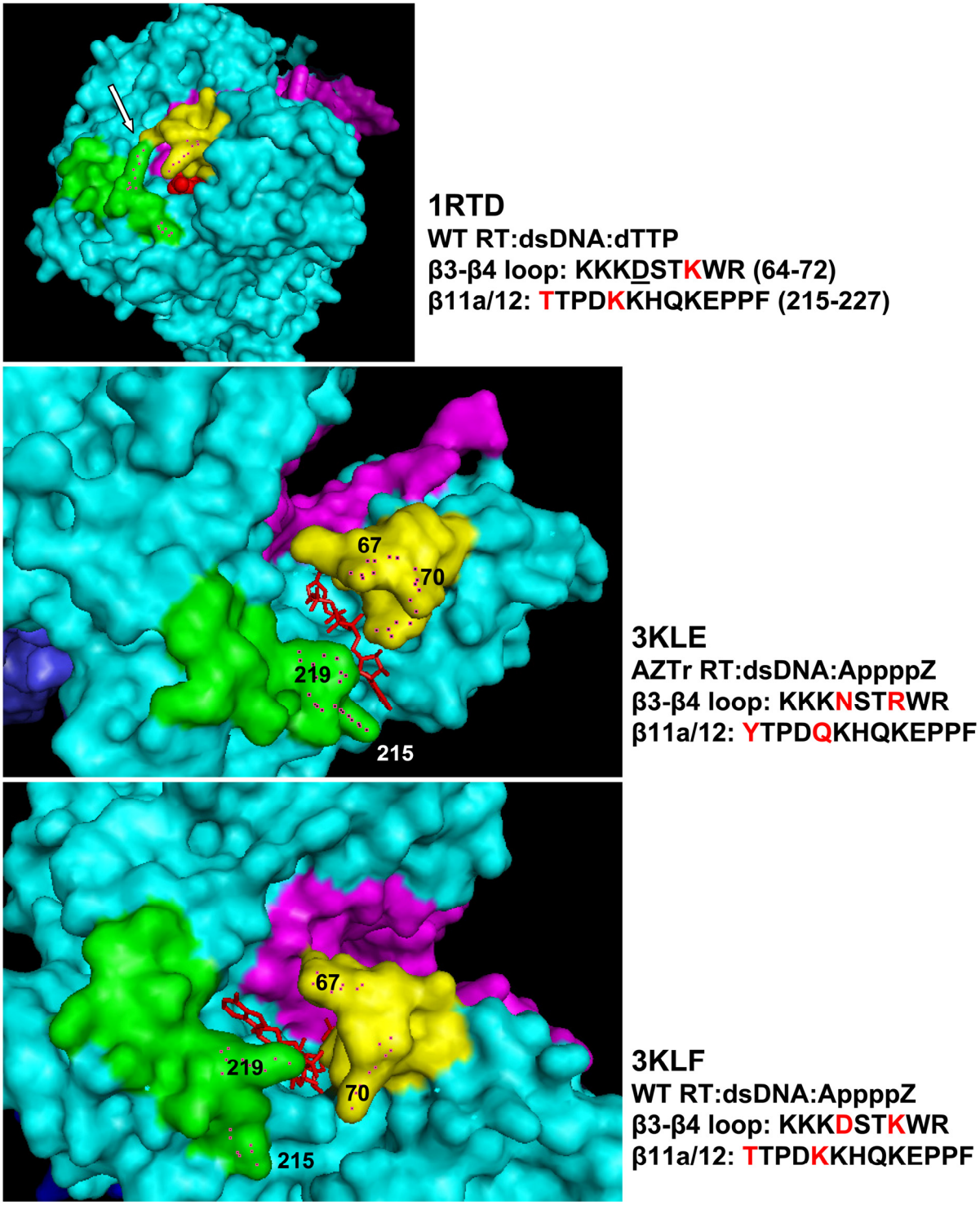

Supplementary Figure S4. Crystal structures of HIV-1 RT complexes showing the location of residues 67, 70, 215 and 219 on the surface of the p66 subunit. *(Top)* Ternary complex of HIV-1 RT, double-stranded (dsDNA) and dTTP (PDB file 1RTD). The arrow indicates the location of the salt bridge between the side-chains of Asp67 and Lys219. *(Middle)* Complex of the AZT-resistant RT (M41L/D67N/K70R/T215Y/K219Q), dsDNA and the dinucleotide tetraphosphate product of the ATP-mediated excision of AZT (AppppZ). *(Bottom)* Complex of the WT RT, dsDNA and the dinucleotide tetraphosphate product of the ATP-mediatend excision of AZT. Surface colors are: cyan (for p66), magenta (for dsDNA), yellow (for β3-β4 hairpin loop residues in p66), green (for residues 215 to 227 of the 66-kDa subunit) and red (for the incoming dTTP). Sticks are used to represent the AppppZ molecule.